CHAPTER THREE

Sequence-Specific Bis-Intercalators

The text of this chapter was taken in part from a manuscript co-authored with Bogdan Olenyuk and Professor Peter B. Dervan (Caltech).

Fechter EJ, Olenyuk B, Dervan PB; Design of a Sequence-Specific DNA Bis-Intercalator, *Angew. Chem. Int. Ed.* **2004**, 43, 3591-3594.

Abstract

Sequence-specific DNA intercalators could potentially inhibit the formation of any target transcription factor:DNA complex without disrupting additional regions of the double helix. To extend our program on generating site-specific intercalators using polyamide conjugates, a bis-intercalator polyamide was designed. Guided by the results in Chapter two, an H-pin polyamide was linked to two acridine intercalators and shown to bind a target DNA site with high affinity and specificity. The molecule has an affinity more than 10-fold higher than a mono-acridine control polyamide and more than 400-fold higher than a control lacking acridine, suggesting each acridine intercalator contributes to overall binding. The bis-acridine conjugate unwinds DNA by roughly twice that of the mono-acridine control and demonstrates a greater propensity to disrupt a GCN4:DNA complex. This design represents a highly specific DNA binding molecule capable of large allosteric distortions in the DNA and may be valuable in studies on regulating gene expression.

Introduction

The development of sequence-specific DNA bisintercalators has been an ongoing challenge in the field of bioorganic chemistry and molecular recognition. Since the first proposed model of intercalation by Lerman in 1963[1], the disruption of transcription or replication by helix unwinding and extension has become an attractive strategy for blocking essential gene functions in the field of cancer therapy and antibiotics but has proven toxic presumably due to lack of specificity (Figure 3.1a).[2,3] By the mid 1970's, Waring and others reported the DNA-binding characteristics of the first known bisintercalating natural product, echinomycin[4-7] (Figure 3.1b). This pseudo-symmetrical bifunctional molecule is part of a larger class, known as quinoxaline antibiotics, and contains a cyclic octapeptide minor groove-binding region with two linked chromophores capable of simultaneous intercalation.[8] The minor groove-binding bicyclic depsipeptide backbone hydrogen bonds to DNA bases and were thought to impose the modest sequence specificity for poly(dG-dC) sites.[4-7] Similarly, the related bisintercalator triostin[9,10] also inhibits DNA replication and RNA synthesis[11] yet has a slight specificity toward poly(dA-dT) sites.[12] As with other members of the quinoxaline family of antibiotics, the incorporation of modified amino acids presumably provide their relative specificities.

Synthetic bisintercalators were later constructed by linking two heterocycles, such as acridines,[13,14] methidium,[15] and anthracyclines[16] with chains of varying lengths to maximize the bracketing of two (or more) base pairs between the intercalator sites (Figure 3.1c). In general, these molecules have enhanced affinity for DNA but lack significant sequence specificity. To our knowledge, in the past 30 years, attempts to design bisintercalators with programmable sequence specificity have been largely unsuccessful.

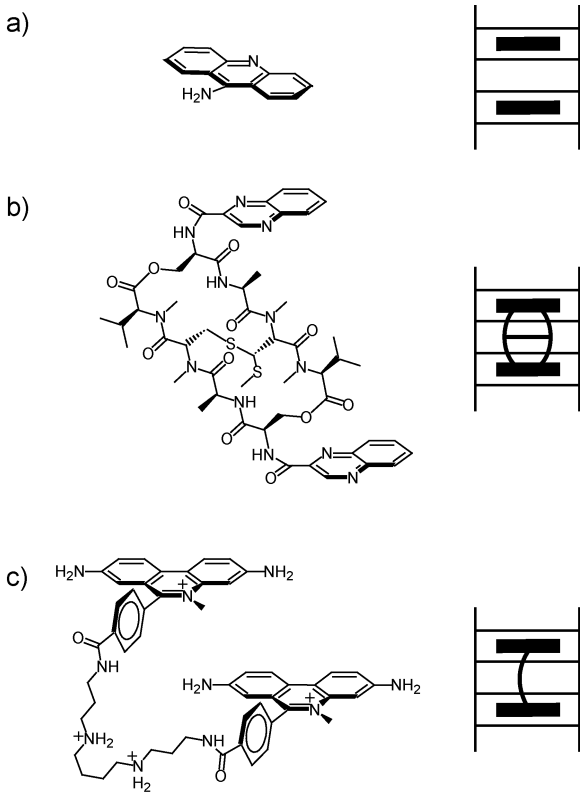

Figure 3.1 Intercalative models: molecular structures (left) and binding models (right). (a) 9-aminoacridine[1] (b) echinomycin[4-7] (c) bis(methidium)spermine.[15]

Chapter two reports synthesis of a hybrid molecule – a hairpin polyamide-acridine conjugate – which enforces two very different modes of DNA binding: groove binding and intercalation.[17] Remarkably, the pyrrole-imidazole polyamide, which prefers to bind B-form DNA, maintains its sequence specificity despite the presence of an adjacent intercalated acridine which extends and unwinds the helix (unwinding angle ϕ = 14-15^{o}) proximal to the groove binding ligand.[17]

Based on this sequence-specific intercalator lead[18] we explored the synthesis and binding properties of sequence-specific bisintercalators (Figure 3.2). Our design is a two-fold symmetric molecule that contains a minor groove-binding polyamide based on the H-pin motif[19] with an acridine moiety at each C-terminus. According to the pairing rules,[20] the H-

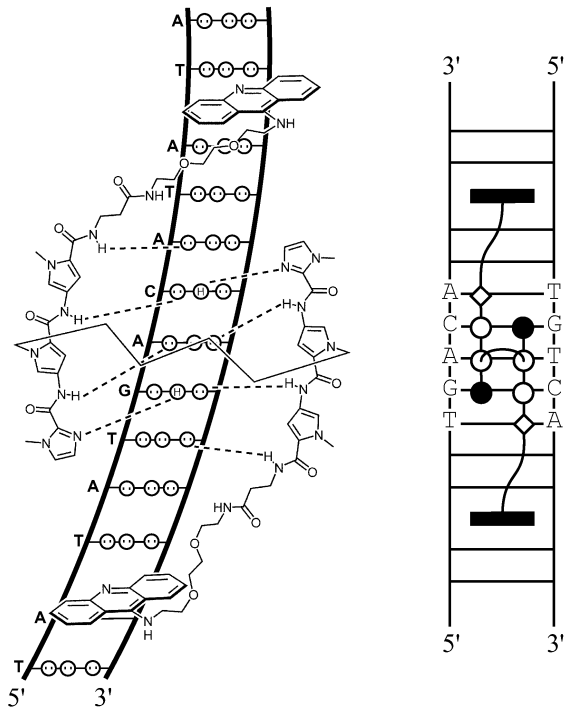

Figure 3.2 DNA binding model for the two-fold symmetric bisintercalating H-pin polyamide-acridine conjugate (ImPyPy-β-Do-Acr)$_2$(CH$_2$)$_6$ bound to the minor groove of 5'-TGACA-3'. (Left) Circles with dots represent lone pairs of N3 of purines and O2 of pyrimidines. Circles containing an H represent the N2 hydrogens of guanine. Putative hydrogen bonds are illustrated by dotted lines. (Right) Solid circles represent imidazoles (Im), open circles represent pyrroles (Py), and diamonds denote β-alanine (β). The shaded bars depict the acridine intercalators. According to the pairing rules, Im/Py codes for G•C, Py/Py for A•T or T•A, Py/Im for C•G, and β-alanine for A,T.

pin core should target the sequence 5'-TGACA-3' and, based on earlier precedent, two acridines should unwind DNA by $\geq 30^{o}$ degrees.

Results

Synthesis of Polyamide-Acridine H-pin Conjugates

Cross-linked resin **1** was synthesized by loading β-Ala-PAM resin with activated pyrrole amino acid[21] followed by Boc deprotection and addition of the ring-linked dimeric building block to couple the C-termini of the growing polyamide chain on resin.[19] A final capping reaction using activated imidazole carboxylate (Figure 3.3) afforded **1**. Resin-bound

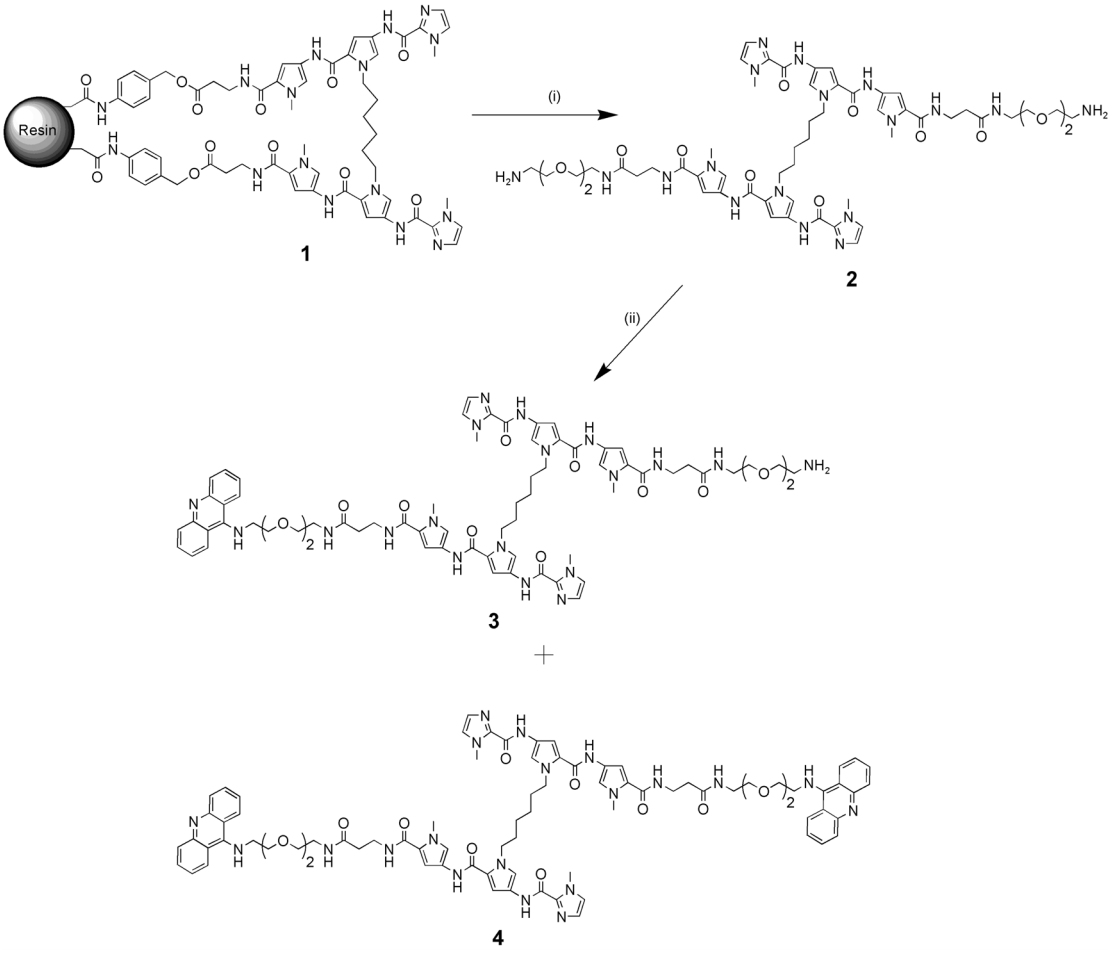

Figure 3.3 Synthetic scheme for polyamide-acridine H-pin conjugates: (i) 2,2'-(ethylenedioxy)-bis(ethylamine), 55 ^{o}C (18 h); (ii) 9-chloroacridine (1.5 eq.), DIEA, 100 ^{o}C (1.5 h).

H-pin **1** was then subjected to aminolytic cleavage with 2,2'-(ethylenedioxy)bis(ethylamine) to form H-pin diamine **2**. Following purification, H-pin **2** was coupled with 9-chloroacridine under reported conditions[17] to produce the mono- and bis- acridine H-pin conjugates **3** (ImPyPy-β-Do-Acr)(ImPyPy-β-Do)$(CH_2)_6$ and **4** (ImPyPy-β-Do-Acr)$_2(CH_2)_6$, respectively.

Binding Energetics and Sequence Specificity

DNA-binding properties of **2**-**4** were investigated by quantitative DNase I footprinting assays[22] (Figure 3.4). The 5'-^{32}P-labeled PCR-amplified fragment of pEF12 (Figure 3.4a) contains a match site (**A**) and a single bp mismatch site (**B**) used to study both

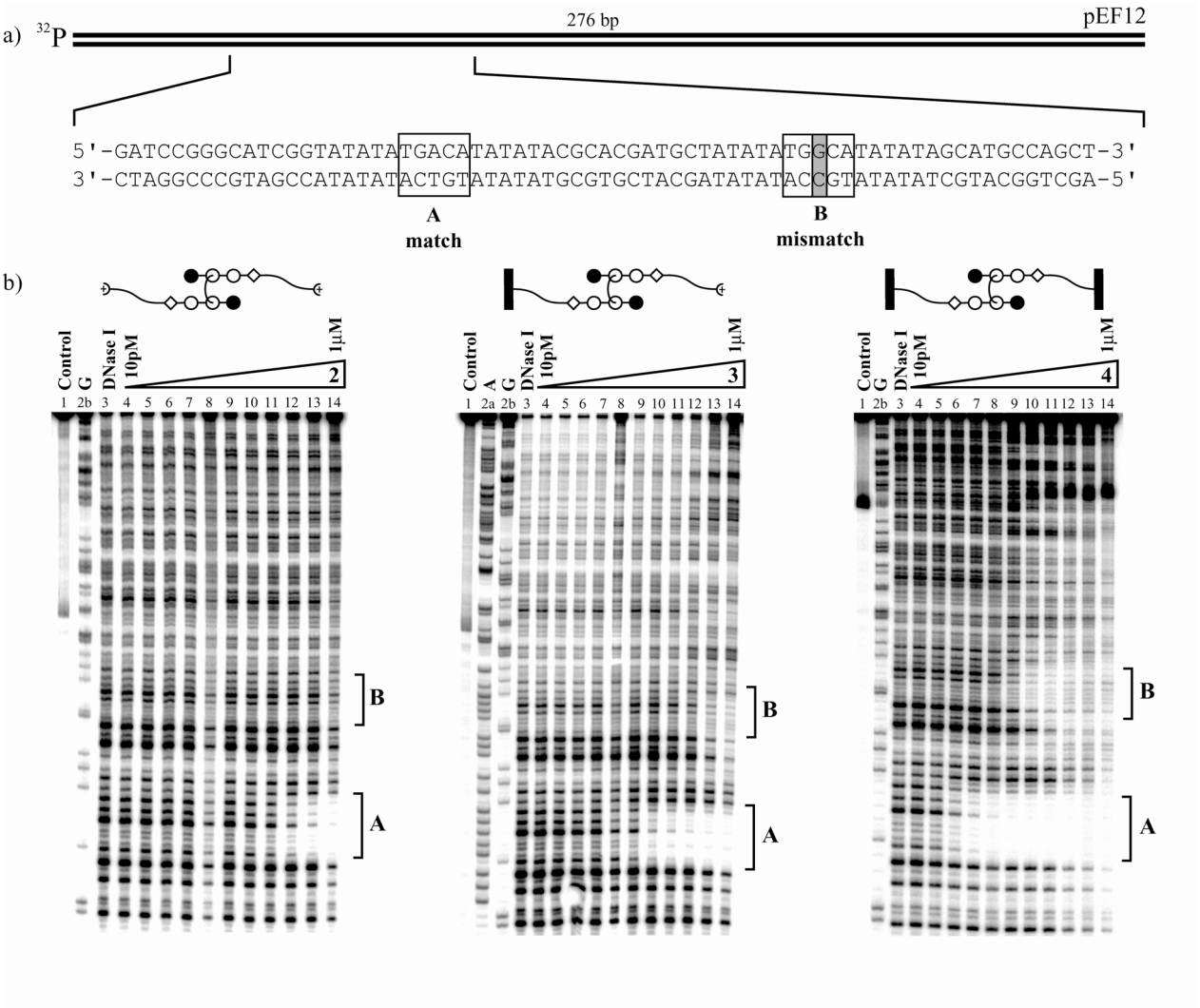

Figure 3.4 (a) Sequence of the synthesized insert from the pEF12 plasmid containing the 5-bp target match site (**A**) and single bp mismatch site (**B**). Target sites are shown in boxes with the mismatch site shaded. (b) Quantitative DNase I footprint titration experiments with H-pins **2** (left), **3** (middle), and **4** (right) on the PCR-amplified 5'-^{32}P-labeled fragment from pEF12. Lane 1, intact DNA; lane 2a, A reaction; lane 2b, G reaction; lane 3, DNase I standard; lanes 4-14, DNase I digestion products in the presence of 10, 30, 100, 300 pM; 1, 3, 10, 30, 100, 300 nM; and 1 uM polyamide, respectively.

affinity and specificity. The equilibrium binding constants of compounds **2**-**4** for match site (**A**) (5'-TGACA-3') are compiled in Table 3.1, and their corresponding binding isotherms are shown in Figure 3.6a. Conjugation of a single acridine (**3**) results in a nearly 40-fold increase in binding affinity (K_a = 1.4 × 10^9 M^{-1}) over the parent H-pin **2** (K_a = 3.7 × 10^7 M^{-1}). The conjugation of a second acridine intercalator (**4**) increases the binding affinity by an

additional 10-fold (K_a = 1.5 × 10^{10} M^{-1}), resulting in the bisacridine conjugate **4** having more than 400 times higher affinity for a DNA match site than its unconjugated counterpart **2**. It is noteworthy that polyamides conjugated to non-intercalating moieties (such as fluorescent dyes and peptides) display *decreased* binding affinities relative to their parent, unconjugated compounds.[23,24] The steep slopes of isotherms **3** and **4** in Figure 3.6a suggest a more complex DNA binding mode than the expected one-to-one association of parent H-pin **2**. Compounds **2** and **3** show no binding on mismatch site (**B**) (5'-TG**G**CA-3') at concentrations as high as 1μM. It appears that bisintercalator **4** may have a partial occupation to the mismatch site (**B**) at the highest concentrations (Figure 3.4b). Nonetheless, the affinity of H-pin **4** for mismatch site (**B**) could not be quantitated at concentrations as high as 1μM, indicating a high level of specificity for this series of conjugates.

Helical Unwinding Angle Determination

The DNA-unwinding properties of compounds **3** and **4** were determined from a helical assay developed by Crothers and Zeeman capable of providing an unwinding angle (ϕ) from sequence-specific interactions.[25,26] A series of relaxation reactions were carried out using topoisomerase I (Topo I) on closed-circular pUC19 DNA pre-equilibrated with varying concentrations of polyamides. The plasmid was then separated from polyamide conjugate by phenol:chloroform extraction and run on two-dimensional (2D) agarose gel electrophoresis to distinguish the

Table 3.1 Thermodynamic Data and Unwinding Angles

polyamide	# of Acridines	K_a [a] (M^{-1})	ϕ (degrees)
2	0	3.7 x 10^7	0
3	1	1.4 x 10^9	15
4	2	1.5 x 10^{10}	34

[a] Association constants are the average values obtained from at least three DNase I footprint titration experiments. Assays were performed at 22°C at pH 7.0 in the presence of 10 mM Tris●HCl, 10 mM KCl, 10 mM $MgCl_2$, and 5 mM $CaCl_2$.

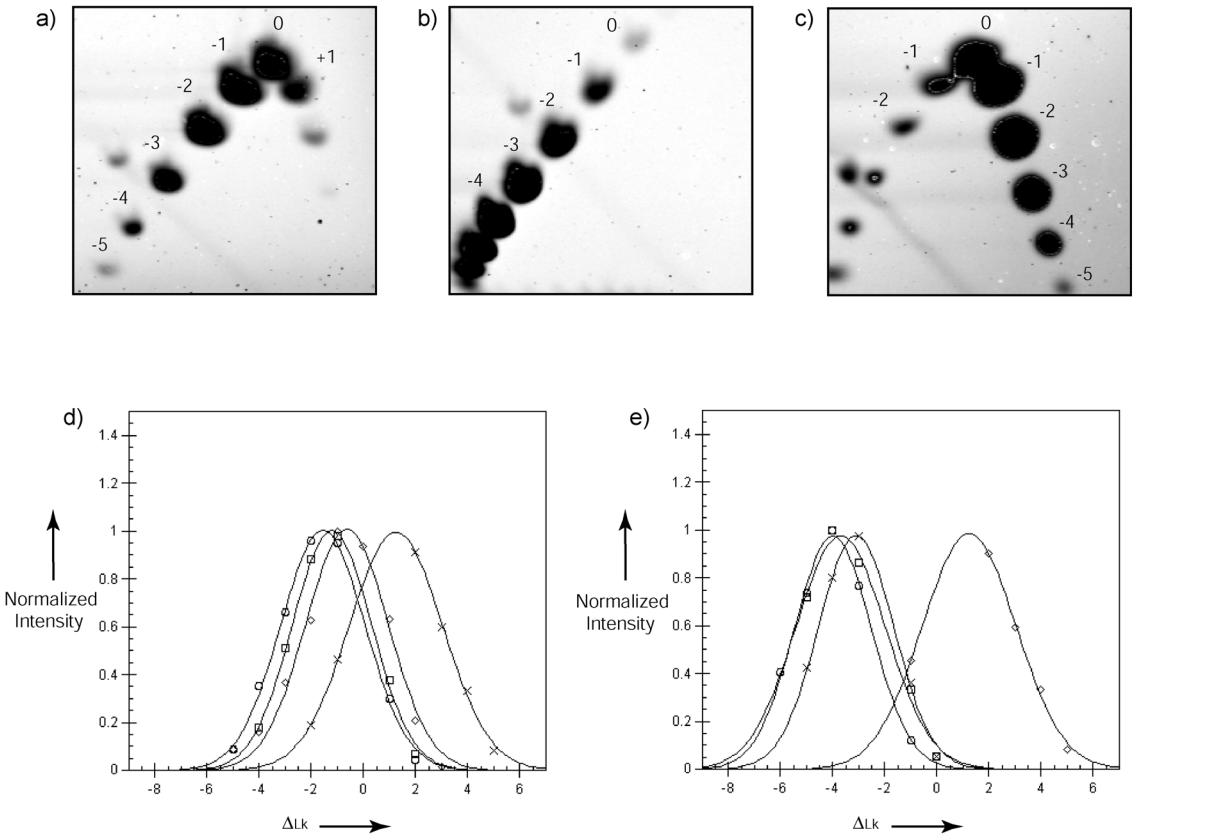

Figure 3.5 (Top) Representative images of topoisomer bands from reactions containing equal volume of a) polyamide-acridine conjugate **3**, b) polyamide-bisacridine conjugate **4**, and c) no polyamide. Each ΔLk number is indicated. (Bottom) Three normalized Boltzman distributions with varying volumes of d) polyamide-acridine conjugate **3**, and e) polyamide-bisacridine conjugate **4**. The right-most distribution in both d) and e) represents controls lacking polyamide.

resulting distribution of topoisomers (Figure 3.5). DNA unwinding would shift the topoisomer distribution toward a more negatively supercoiled population. Indeed, each reaction containing conjugate **4** had a more highly negative distribution of topoisomers than those containing conjugate **3** (Figure 3.5). Control experiments lacking polyamide resulted in a primarily positive distribution of topoisomers. Mathematical analysis of the topoisomers distributions relative to the controls showed decreasing apparent unwinding angles (ϕ_{ap}) for simultaneously decreasing conjugate and plasmid concentrations (Figure 3.6b). The actual

unwinding angles (ϕ) determined from the ordinate intercepts are 15° and 34° for the acridine conjugate **3** and bis-acridine conjugate **4**, respectively (Figure 3.6b).

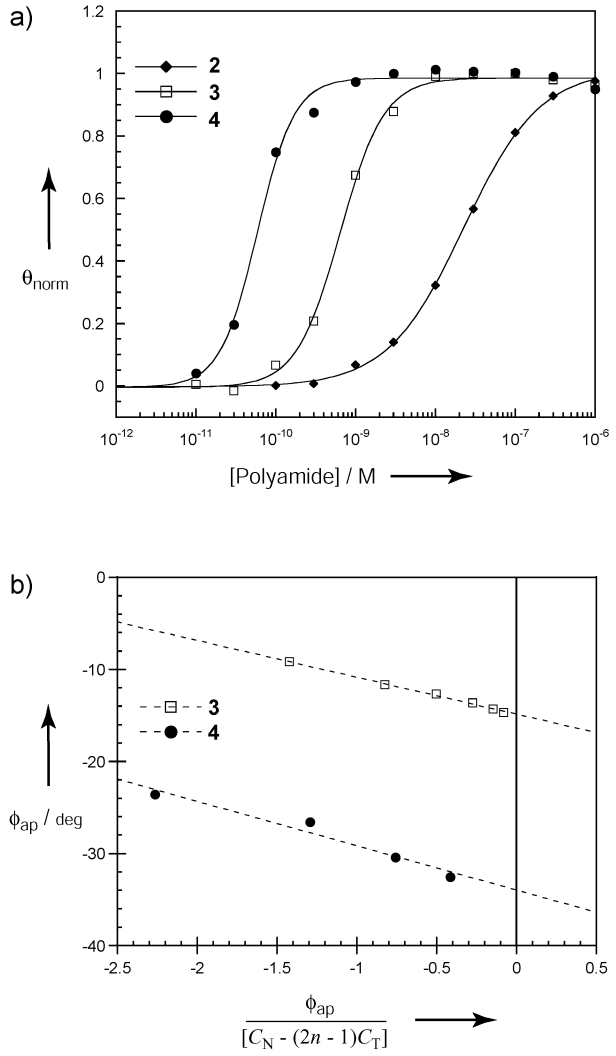

Figure 3.6 (a) Binding isotherms at match sites for H-pins **2**, **3**, and **4**. θ_{norm} points were obtained using storage phosphor autoradiography and processed by standard methods.[15] Each data point shows the average value obtained from three footprinting experiments. The solid curves are best-fit Langmuir binding titration isotherms obtained from nonlinear least squares algorithm. (b) Binding isotherms for polyamide-acridine conjugates **3** and **4** on pUC19. Each data point was calculated from one set of topoisomer distributions from reactions containing polyamide compared to a control distribution lacking polyamide. Interception of the ordinate yields the unwinding angle (ϕ) per polyamide-acridine conjugate.

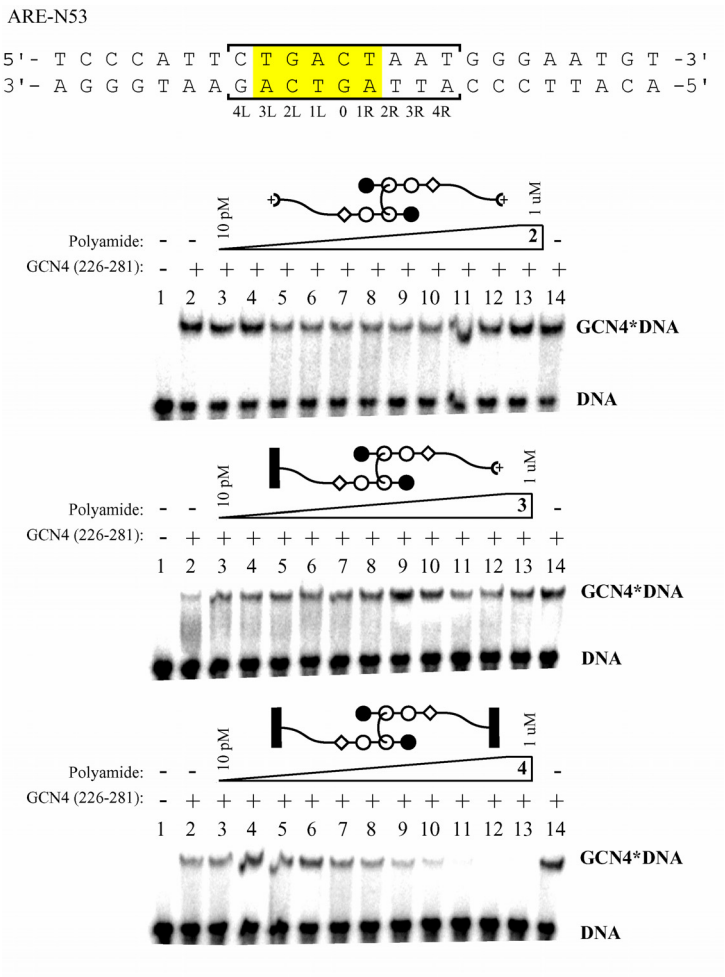

Figure 3.7 Representative GCN4 (222-281) electrophoretic mobility shift assay results for conjugates **2**, **3**, and **4** with ARE-N53. The pseudopalindromic GCN4 binding site is shown in brackets and the base pair assignments shown below the duplex. The polyamide binding site is shown as a yellow box. The storage phosphor autoradiograms of **2-4** are shown below the duplex. Upper band, GCN4 (222-281)-DNA complex; lower band, free DNA; lane 1, DNA only; lane 2, DNA incubated with 300 nM GCN4 (222-281); lanes 3, 4, 5, 6, 7, 8, 9, 10, 11, 12, and 13 are 300 nM GCN4 (222-281) and 10 pM, 30 pM, 100 pM, 300 pM, 1 nM, 3 nM, 10 nM, 30 nM, 100 nM, 300 nM, and 1 μM **2**, **3**, or **4**, respectively; lane 14, DNA incubated with 300 nM GCN4 (222-281).

Effects of Polyamide-Acridine Conjugates on Major-Groove Protein-DNA Complex Formation

The polyamide-acridine conjugates were then tested for their abilities to selectively inhibit the association GCN4 (222-281) homodimer to DNA.[27-29] Inhibition was determined by performing an EMSA of the ^{32}P radiolabeled 33-bp DNA duplex, ARE-N53, containing the GCN4-binding site (5'-CTGACTAAT-3')[30,31] and a match site for the designed conjugates

(5'-WGWCW-3'). Representative gels show lack of shifted bands from complexed to free DNA for compounds **2** and **3** as the conjugate concentrations were increased from 10pM to 1μM in the presence of 300 nM concentration of GCN4 (Figure 3.7). However, the bis-acridine conjugate **4** showed quantitative inhibition and an IC_{50} values of ~3 nM.

Since the polyamide binding site is symmetrical, the polyamide can theoretically bind in one of two orientations. The mono-acridine conjugate **3** likely binds in the energy minimized orientation, which projects its single intercalator outside of the protein binding region to allow co-occupancy of polyamide and GCN4. With the binding of bis-acridine **4**, the ligand is forced to intercalate at both locations despite the orientation, creating a distortion that is incompatible with GCN4 binding.

Our results provide strong evidence that the two-fold symmetric H-pin-bisacridine conjugate **4** is a sequence-specific bisintercalator capable of binding discrete sites at subnanomolar concentrations and unwinding DNA by more than 30^{o}. To date, this synthetic molecule exceeds the specificity and binding affinity of any known natural or unnatural bisintercalator. Additionally, this conjugate design surpasses the potency for specific GCN4 complex inhibition when compared to previously synthesized polyamide-intercalator hybrids. Its ease of synthesis, sequence specificity, and potency of DNA distortion at discrete sites make it an attractive candidate for future biological studies such as transcription inhibition at specific genes. The design features of combining the programmable H-pin motif with intercalation should allow a large repertoire of discrete DNA sequences to be targeted.

Experimental

Materials

9-Chloroacridine was purchased from Pfaltz & Bauer, Inc. Restriction endonucleases were purchased from New England Biolabs and used as noted in the manufacturer's protocol. Sequenase (version 2.0) was obtained from Boeringher-Mannheim. [α-^{32}P]-Thymidine-5'-triphosphate (≥3000 Ci/mmol) and [α-^{32}P]-deoxyadenosine-5'-triphosphate (≥6000 Ci/mmol) were purchased from DuPont/NEN. [γ-^{32}P]-Adenosine-5'-triphosphate (≥6000 Ci/mmol) was obtained from ICN. Purified pUC19 DNA for unwinding angle determination was isolated from transformed JM109 *Escherichia coli* using the Qiagen protocol. EDTA, dithiothreitol (DTT), ultrapure agarose, and calf thymus Topo I were purchased from GIBCO/BRL. Micron 50 microconcentrators were purchased from Amicon. ProbeQuant G-50. Micro Columns were purchased from Amersham Pharmacia Biotech, Inc. GCN4 (222-281) prepared by solid-phase synthesis was generously provided by Martha G. Oakley. Water (18 MΩ) was obtained from a Millipore MilliQ water purification system, and all buffers were 0.2 μm filtered. Reagent-grade chemicals were used as received unless otherwise stated.

UV spectra were measured on a Beckman-Coulter DU7400 diode array spectrophotometer. Matrix-assisted, laser desorption/ionization time-of-flight mass spectrometry (MALDI-TOF) was performed using an Applied Biosystems Voyager DE-Pro. HPLC analysis was performed on a Beckman Gold system using a RAININ C_{18}, Microsorb MV, 5 μm, 300 × 4.6 mm reversed-phase column in 0.1% (v/v) TFA with acetonitrile as eluent and a flow rate of 1.0 mL/min. Preparatory reversed-phase HPLC was performed on a Beckman HPLC using a Waters DeltaPak 25 × 100 mm, 100 μm C_{18} column equipped with a guard, 0.1% (wt/v) TFA, 0.25% acetonitrile/min.

(ImPyPy-β-Do)$_2$(CH$_2$)$_6$ (2)

(ImPyPy-β-Do-resin)$_2$(CH$_2$)$_6$ (**1**) was generated from Boc-β-alanine Pam resin (1 g, 0.59 mmol/g) using previously described Boc-protected monomers and methods.[19] A sample of (ImPyPy-β-Do-resin)$_2$(CH$_2$)$_6$ (**1**) (90 mg, 0.356 mmol/g) was suspended in 2,2'-(ethylenedioxy)bis(ethylamine) and heated at 55°C for 12 h. The reaction mixture was filtered to remove resin, 0.1% (wt/v) TFA added (8 mL), and the resulting solution purified by reversed-phase HPLC. (ImPyPy-β-Do)$_2$(CH$_2$)$_6$ (**2**) was recovered upon lyophilization of the appropriate fractions as a yellow powder (8 mg, 21% recovery). MALDI-TOF-MS (monoisotopic) calcd for $C_{67}H_{90}N_{23}O_{15}$ (M+H): 1197.4. Found: 1197.6.

(ImPyPy-β-Do-Acr)(ImPyPy-β-Do)(CH$_2$)$_6$ (3) and **(ImPyPy-β-Do-Acr)$_2$(CH$_2$)$_6$ (4)**

(ImPyPy-β-Do)$_2$(CH$_2$)$_6$ (**2**) (1μmol) was added to 100 μL of phenol and dissolved by heating to 100°C. To this solution was added 9-chloroacridine (0.5 M, 5 μL) in DMF, followed by 10 μL of DIEA, and the reaction was allowed to proceed at 100°C for 1 h. The mixture was then cooled to 50°C and diluted with 0.1% (wt/v) TFA (7mL) and the resulting solution purified by reversed-phase HPLC. Lyophilization of appropriate fractions provided (ImPyPy-β-Do-Acr)(ImPyPy-β-Do)(CH$_2$)$_6$ (**3**) as a yellow powder (0.25 mg, 38% recovery, MALDI-TOF-MS (monoisotopic) calcd for $C_{71}H_{81}N_{24}O_{12}$ (M+H): 1374.6. Found: 1374.8) and (ImPyPy-β-Do-Acr)$_2$(CH$_2$)$_6$ (**4**) as a yellow powder (0.19 mg, 25% recovery, MALDI-TOF-MS (monoisotopic) calcd for $C_{71}H_{81}N_{24}O_{12}$ (M+H): 1551.8. Found: 1551.7).

Construction of Plasmid DNA

The plasmid **pEF12** was constructed by insertion of the following hybridized inserts into the *Bam*HI/*Hind*III polycloning sites in pUC19: 5'- GATCC GGGCA TCGGT ATATA

TGACA TATAT ACGCA CGATG CTATA TATGG CATAT ATAGC ATGCC -3' and 5'-AGCTG GCATG CTATA TATGC CATAT ATAGC ATCGT GCGTA TATAT GTCAT ATATA CCGAT GCCCG -3'. The insert was obtained by annealing complementary *Hind*III restriction fragments of pUC19 using T4 DNA ligase. The ligated plasmid was then used to transform JM109 subcompetent cells (Promega). Colonies were selected for α-complementation on 25 mL Luria-Bertani agar plates containing 50 mg/mL ampicillin. Cells were harvested after overnight growth at 37°C. Large-scale plasmid purification was performed using WizardPlus Midi Preps from Promega. The presence of the desired insert was determined by dideoxy sequencing.

Preparation of 5'-End-Labeled Fragments

Two 21 base-pair primer oligonucleotides, 5'-GAATT CGAGC TCGGT ACCCG G-3' (forward) and 5'-TGGCA CGACA GGTTT CCCGA C-3' (reverse) were constructed for PCR amplification. The forward primer was radiolabeled using [γ-^{32}P]-dATP and polynucleotide kinase, followed by purification using MicroSpin G-50 columns. The desired DNA segment was amplified as previously described.[22] The labeled fragment was loaded onto a 7% nondenaturing preparatory polyacrylamide gel (5% cross-link), and the desired 276 base-pair band was visualized by autoradiography and isolated. Chemical sequencing reactions were performed according to published protocols.[32,33]

Quantitative DNase I Footprint Titrations

All reactions were carried out in a volume of 400 μL according to published protocols.[22] Quantitation by storage phosphor autoradiography and determination of equilibrium association constants were as previously described.[22]

Gel Mobility Shift Assay

Radiolabeled synthetic DNA (5'-AATTC GTATT CCCAT TCTGA CTAAT GGGAA TGTAC C-3') annealed with its complementary strand containing a four base 5' overhang was prepared for gel mobility shift assay by treating with Sequenase (version 2.0), [α-^{32}P]-thymidine-5'-triphosphate, and [α-^{32}P]-deoxyadenosine-5'-triphosphate for 3'-end labeling. The labeled duplex was purified using ProbeQuant G-50 Micro Columns. Polyamide was incubated with the duplex (20,000 cpm) in 40 μL reaction volumes of bisTris (10 mM, pH 7.0), NaCl (100 mM), DTT (1 mM), EDTA (1 mM), and poly(dI-dC)·poly(dI-dC) (5 μg/mL) for 16 h at 22 ^{o}C. GCN4 (222-281) was added and equilibrated for 45 min. Loading buffer (15% Ficoll, 0.025% bromophenol blue, 10 μL) was added, and 10 μL was immediately loaded onto a running 8% (29:1 acrylamide:bis-acrylamide) polyacrylamide gel (0.5 · TBE, 280 V, 0.8 mm, 13 cm). Separation of uncomplexed DNA and DNA-GCN4 (222-281) complexes was achieved within 40 min. Gels were dried in vacuo at 80^{o}C and then exposed to a storage phosphor screen (Molecular Dynamics).[34]

Unwinding Angle and Intrinsic Association Constant Determination

Relaxation reactions and numeric analyses were all carried out as described.[25,26] Minor variations to published protocols include two-dimensional gel electrophoresis carried out in 18 × 20 cm 1% agarose casting units and imaged after ethidium bromide staining with a Typhoon 8600 variable mode imager and 610-nm band-pass filter. The Boltzman distribution of adopted integer Lk values were plotted using equation (1),

$$I = I_{\mathrm{M}} \mathrm{e}^{[-w(\Delta Lk - \Delta Lk_c)^2]} \quad , \qquad (1)$$

where ΔLk and ΔLk_c are the measured linking difference and most abundant linking difference, respectively, I and I_M are integrated and maximum band intensity, respectively, and w is the distribution width. The apparent unwinding angle was calculated using equation (2),

$$\phi_{ap} = \frac{360N_D(\Delta Lk_c - \Delta Lk^o_c)}{N_L} , \qquad (2)$$

where ΔLk^o_c is the most abundant linking difference for the control reactions containing no polyamide and N_D and N_L are the number of pUC19 and polyamide conjugate molecules, respectively. The actual unwinding angle was calculated using equation (3),

$$\phi_{ap} = \phi - \frac{\phi_{ap}}{K_a[C_N - (2n - 1)C_T]} , \qquad (3)$$

where n represents the number of binding sites covered by one conjugate (set to unity) and C_N and C_T represent the concentration of conjugate binding sites and the concentration of polyamide conjugate, respectively. The C_N value was approximated from 268 conjugate binding sites (and single base-pair mismatch sites) per ccDNA molecule for both **3** and **4**. The value of C_N affects the slope in Figure 3.6b but does not influence the value of ϕ (ϕ is the ordinate intercept).

Acknowledgment

We thank the National Institutes of Health (GM-27681) for research support, a Research Service Award to E.J.F., and a postdoctoral fellowship to B.O. (F32 GM-19788). We also thank the Ralph M. Parsons Foundation for a predoctoral fellowship to E. J. F.

References

1. Lerman, L. S., *J. Mol. Biol.* **1961**, 3, 18-30.
2. Denny, W. A., *Anti-Cancer Drug Des.* **1989**, 4, 241-263.
3. Baguley, B. C., *Anti-Cancer Drug Des.* **1991**, 6, 1-35.
4. Waring, M. J. and L. P. G. Wakelin, *Nature* **1974**, 252, 653-657.
5. Wakelin, L. P. G. and M. J. Waring, *Biochem J.* **1976**, 157, 721-740.
6. Shafer, R. H. and M. J. Waring, *Biopolymers*, **1980**, 19, 431-443.
7. Van Dyke, M. M. and P. B. Dervan, *Science* **1984**, 225, 1122-1127.
8. Dell, A., D. H. Williams, H. R. Morris, G. A. Smith, J. Feeney, and G. C. K. Roberts, *J. Am. Chem. Soc.* **1975**, 97, 2497-2502.
9. Wang, A. H. J., G. Ughetto, G. J. Quigley, T. Hakoshima, G. A. van der Marel, J. H. van Boom, and A. Rich, *Science* **1984**, 225, 1115-1121.
10. Chen, H. and D. J. Patel, *J. Mol. Biol.* **1995**, 246, 164-179.
11. Ward, D. C., E. Reich, and I. H. Goldberg, *Science* **1965**, 149, 1259-1263.
12. Lee, J. S. and M. J. Waring, *Bichem. J.* **1978**, 173, 115-128.
13. Le Pecq, J. -B., M. Le Bret, J. Barbet, and B. Roques, *Proc. Nat. Acad. Sci.USA* **1975**, 72, 2915-2919.
14. Wakelin, L. P. G., M. Romanos, T. K. Chen, D. Glaubiger, E. S. Canellakis, and M. J. Waring, *Biochemistry* **1978**, 17, 5057-5063.
15. Becker, M. M. and P. B. Dervan, *J. Am. Chem. Soc.* **1979**, 101, 3664-3666.
16. Leng, F., W. Priebe, and J. B. Chaires, *Biochemistry* **1998**, 37, 1743-1753.
17. Fechter, E. J. and P. B. Dervan, *J. Am. Chem. Soc.* **2003**, 125, 8476-8485.

18. For an example of a major groove sequence specific intercalator see: Kielkopf, C. L., K. E. Erkkila, B. P. Hudson, J. K. Barton, and D. C. Rees, *Nature Struct. Biol.* **2000**, 7, 117-121.

19. Olenyuk, B., C. Jitianu, and P. B. Dervan, *J. Am. Chem. Soc.* **2003**, 125, 4741-4751.

20. White, S., J. W. Szewczyk, J. M. Turner, E. E. Baird, and P. B. Dervan, *Nature* **1998**, 391, 468-471.

21. Baird, E. E. and P. B. Dervan, *J. Am. Chem. Soc.* **1996**, 118, 6141-6146.

22. Trauger, J. W. and P. B. Dervan, *Methods Enzymol.* **2001**, 340, 450-466.

23. Best, T. P., B. S. Edelson, N. G. Nickols, and P. B. Dervan, *Proc. Natl. Acad. Sci USA.* **2003**, 100. 12063-12068.

24. Mapp, A. K., A. Z. Ansari, M. Ptashne, and P. B. Dervan, *Proc. Natl. Acad. Sci.* **2000**, 97, 3930-3935.

25. Zeeman, S. M., K. M. Depew, S. J. Danishefsky, and D. M. Crothers, *Proc. Natl. Acad. Sci.USA* **1998**, 95, 4327-4332.

26. Zeeman, S. M. and D. M. Crothers, *Methods Enzymol.* **2001**, 340, 51-68.

27. Ellenberger, T. E., C. J. Brandl, K. Struhl, and S. C. Harrison, *Cell* **1992**, 71, 1223-1237.

28. Keller, W., P. Konig, and T. J. Richmond, *J. Mol. Biol.* **1995**, 254, 657-667.

29. The 60 amino acid sequence (222-281) of GCN4 contains the 'leucine zipper' dimerization domain and the 'basic region' responsible for DNA binding.

30. Oakely, M. G., M. Mrksich, and P. B. Dervan, *Biochemistry* **1992**, 31, 10969-10975.

31. Oakely, M. G. and P. B. Dervan, *Science* **1990**, 248, 847-850.

32. Maxam, A. M. and W. S. Gilbert, *Methods Enzymol.* **1980**, 65, 499-560.

33. Iverson, B. L. and P. B. Dervan, *Methods Enzymol.* **1996**, 15, 7823-7830.

34. Wang, C. C. C., U. Ellervik, and P. B. Dervan, *Bioorg. Med. Chem.* **2001**, 9,653.

35. Johnston, R. F., S. C. Pickett, and D. L. Barker, *Electrophoresis* **1990**, 11, 355-360.